Catalysis Letters (2018) 148:1803–1814
https://doi.org/10.1007/s10562-018-2372-x

Effects of Pressure and Temperature in Hydrothermal Preparation of MoS_2 Catalyst for Methanation Reaction

Jae-Myeong Choi[1] · Sung-Hyun Kim[1] · Seung-Jae Lee[2] · Seong-Soo Kim[2]

Received: 7 February 2018 / Accepted: 24 March 2018 / Published online: 27 April 2018

Abstract
Unsupported MoS_2 catalysts were prepared for the methanation reaction by varying the pressure and temperature in the hydrothermal reaction by using ammonium tetrathiomolybdate (ATTM). The physical and chemical characteristics of the catalysts were analyzed by using XRD, SEM, TEM, BET, XPS, H_2-TPR, and CO-TPD techniques. The catalyst particles were formed in the bent fringe shape by stacking the (0 0 2) planes, and consisted mostly of MoS_2, with some Mo_2S_5 and MoS_3. It was found that the BET surface and active sites such as surface Mo^{4+} and sulfur vacancies increased with increasing preparation pressure, which could contribute to the improvement of MoS_2 catalytic activity. The increase in preparation temperature not only favored the decomposition of ATTM into MoS_2, but also lowered the number of active sites accessible for the reaction. Thus, it was suggested that the preparation temperature should be controlled at 350 °C to improve the catalytic activity.

Graphical Abstract

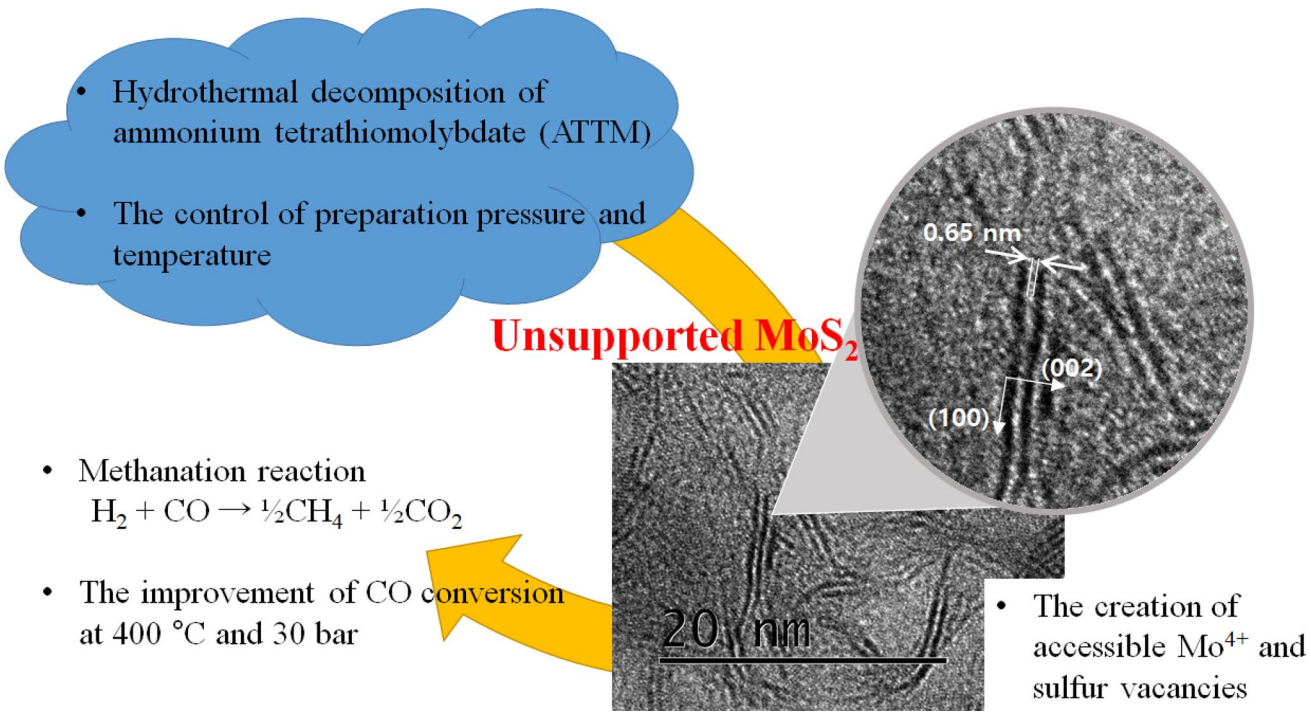

Keywords MoS_2 · Hydrothermal reaction · Pressure · Temperature · Catalytic activity

Extended author information available on the last page of the article

1 Introduction

MoS_2 (molybdenum disulfide) is a typical transition metal dichalcogenide with a layered structure, in which a molybdenum atom layer is sandwiched between two layers of sulfur atoms [1, 2] and the MoS_2 layers hold each other by weak van der Waals interactions [3]. MoS_2 has attracted growing attention due to its structural properties and potential application as a lubricant [4], in lithium ions batteries [5], and as a catalyst in hydrogen evolution (HER) [6], hydrodeoxygenation (HDO) [7], hydrodesulfurization (HDS) [8–12], hydrodenitrogenation (HDN) [13], and hydrogenation (HYD) [14–17] reactions.

The catalytic active sites of MoS_2 have been investigated in various reactions. It has been suggested that the sulfur vacancies generated at the edge planes of a layered MoS_2 structure could be associated with the active sites for HDS [18, 19] and methanation [20]. It was also reported that the lower valence state of the MoS_2 and the number of anion vacancies could contribute to the catalytic activity of MoS_2 for a thiophene hydrogenolysis reaction [21]. In the rim-edge model proposed by Dagge and Chianelli [22], the rim sites are mainly responsible for a HYD reaction and the edge ones for sulfur removal. On the other hand, it was observed that the "inflection" on the basal plane of MoS_2 could be highly active in HYD [23].

Unsupported MoS_2 catalysts can be prepared by several methods such as chemical vapor deposition (CVD) [24], sonochemical synthesis [25], thermal decomposition [26], exfoliation [27, 28], solvothermal synthesis [29], and hydrothermal synthesis [30, 31]. In particular, hydrothermal preparation is much superior to the others in the control of nucleation, particle shape, dispersion, and reaction rate by adjusting temperature and pressure at a low synthesis temperature [32]. A lot of research has examined the effect of temperature on catalyst preparation, whereas that of pressure has been less studied. When MoS_2 was prepared by thermal decomposition at 300 or 350 °C in H_2, the variation of pressure between 30 and 50 bar in the preparation did not significantly affect the catalytic performance in the HDS reaction [33]. In the preparation of MoS_2 using ammonium tetrathiomolybdate (ATTM, or $(NH_4)_2MoS_4$), with the open-flow isostatic pressing method, it was found that the increase in the synthesis pressure from 6.9 to 55.2 bar could improve the catalytic activity in HDS [34]. An in-situ decomposition by heating ATTM to 350 °C at a pressure of 31 bar in an H_2 environment could produce highly disordered MoS_2 and a large surface area, which resulted in enhanced activity in the HDS reaction of dibenzothiophene (DBT) [35]. Furthermore, the stacks of the single MoS_2 layer could be obtained by varying the pressure of hydrothermal synthesis in an autoclave between 170 and 200 °C [36].

Although it has been known that the increase in the pressure in the preparation of MoS_2 can improve the catalytic activity, especially for the HDS reaction, there has not been any systematic study of the effect of preparation conditions on the morphology and the methanation reaction of MoS_2. In this study, unsupported MoS_2 catalysts are hydrothermally prepared at various pressures and temperatures in a continuous flow of H_2 and are then examined for physical and chemical characteristics, and catalytic performance, in the methanation reaction.

2 Experimental

2.1 Catalyst Preparation

The schematic diagram of the hydrothermal reaction system for the preparation of MoS_2 is shown in Fig. 1. ATTM 99.99% from Alfa Aesar was used as the precursor of MoS_2. 5 g of ATTM and 250 mL of doubly distilled water were stirred in a 1 L Inconel 600 cylindrical vessel at 200 rpm for 30 min in 80 mL/min of Ar gas flow, followed by a further 1 h in 30 mL/min of H_2 gas flow. The pressure inside the vessel was increased up to a predetermined value between 5 and 40 bar. The temperature was also controlled to a desired value between 300 and 400 °C. After the hydrothermal reaction, the temperature inside the vessel was cooled down to room temperature for 12 h in 200 mL/min of Ar flow.

2.2 Characterization

The prepared MoS_2 catalysts were subjected to characterization. The content of elemental sulfur was analyzed using a SC-432DR Sulfur Analyzer (LECO Co., USA). The SEM images were obtained using a Zeiss Supra 50VP scanning electron microscope equipped with EDS. The shape of the nano-sized particles was examined using a high-resolution transmission electron microscope (HRTEM, JEOL JEM-2010). The structure of the catalysts was analyzed by Rigaku D/Max-2500 X-ray diffractometer (40 kV, 100 mA) with Cu Kα ($\lambda = 1.5414$ Å) as the radiation source at 2°/min in a range of 2θ between 5° and 90°, and identified using the JCPDS (Joint Committee on Powder Diffraction Standards) library. An X-ray photoelectron spectroscopy (XPS) study was carried out to distinguish the chemical states of Mo and S on the surface of MoS_2 using an Axis Nova spectrometer (Kratos) with a monochromatic Al K_α X-rays source (1486.6 eV), operated at 15 kV and 10 mA under a chamber pressure of 10^{-8} Torr. All binding energies were referenced to that of O 1s (531.0 eV). The baseline corrections for the peak fitting were carried out using the Shirley method. The BET surface area of the sample was determined by measuring N_2 adsorption–desorption

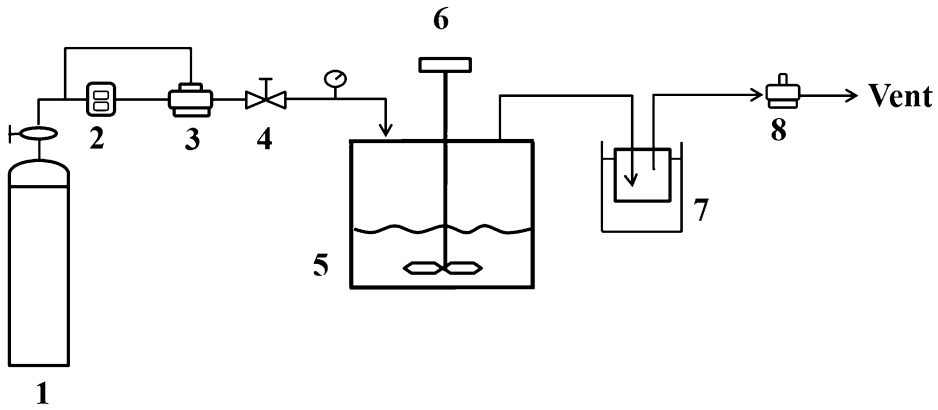

1. H_2 Gas 2. Mass Flow Controller 3. High Pressure Gas Controller 4. Flow Restrictive Valve
5. Reactor 6. Impeller 7. Condenser 8. Back Pressure Regulator

Fig. 1 Schematic of the hydrothermal reaction system for MoS_2 preparation

isotherms at 77 K with the ASAP 2020, Micromeritics Instrument. CO-TPD (temperature programmed desorption), and H_2-TPR (temperature programmed reduction) measurements were performed using Micromeritics AutoChem 2920. In CO-TPD measurements, 100 mg of a sample was pretreated at 250 °C for 1 h in 50 mL/min of He gas flow. After CO adsorption at 400 °C for 3 h in 30 mL/min of 10% CO/He gas flow, a sample was cooled down to room temperature in 40 mL/min of He flow. The TCD signal was collected during CO desorption by heating up to 900 °C at 10 °C/min. For H_2-TPR analysis, 100 mg of sample was pretreated at 120 °C for 1 h in 30 mL/min of Ar gas flow, followed by heating from room temperature to 800 °C at 10 °C/min in 30 mL/min of 10% H_2/Ar gas flow.

2.3 Catalytic Reaction

The prepared MoS_2 catalysts were evaluated in catalytic activity for methanation by using an Inconel 600 cylindrical fixed-bed reactor with an internal diameter of 8 mm and a length of 450 mm, as shown in Fig. 2. 0.5 g of catalyst was placed between two layers of silica wool in the middle of the cylindrical reactor. Two K-type thermocouples were installed above and below the catalyst bed to monitor and control the temperature. The difference in

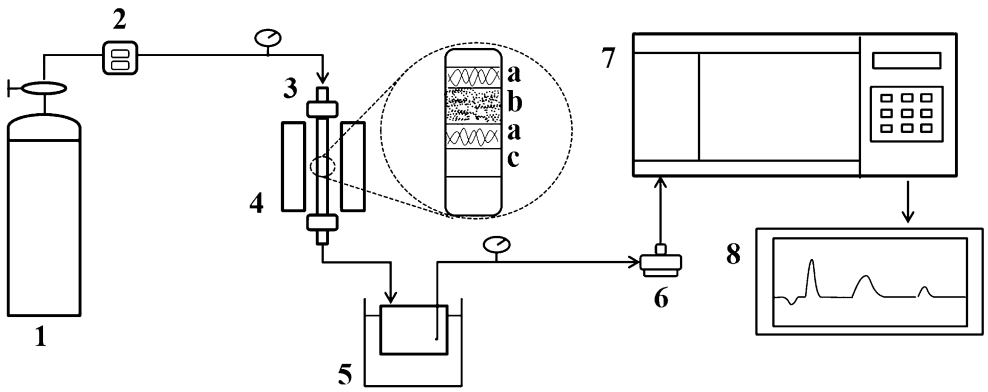

1. Mixture Gas 2. Mass Flow Controller 3. Reactor (a. Glass wool, b. Catalyst, c. Support)
4. Heater 5. Condenser 6. Back Pressure Regulator 7. Gas Chromatograph 8. Computer

Fig. 2 Schematic of the methanation reaction system for evaluation of the catalytic activity of MoS_2

temperature between the two thermocouples was within ± 2 °C. The catalysts were subjected to methanation at 400 °C at 30 bar. The composition of the reactant gas mixture was 50% H_2/50% CO (i.e., a H_2/CO ratio of 1.0). The flow rate of the reactant gas mixture was 80 mL/min, corresponding to the gas hourly space velocity (GHSV) of 4800 h^{-1}. An HP 6890 Series II gas chromatograph using a packed column filled with Carbosphere® was employed for the analysis of the composition of reactant and product gases. The catalytic activity of MoS_2 in the methanation reaction for Eq. (1) was assessed in terms of CO conversion as Eq. (2) [37] under the assumption that the mass balance is satisfied by 100%.

$$H_2 + CO \rightarrow {}^1/_2CH_4 + {}^1/_2CO_2 \quad (1)$$

$$\text{CO conversion (\%)} = \left(\sum n_i V_i / V_{co}\right) \times 100 \quad (2)$$

where n_i is the number of carbon atoms in product *i*, V_i the volume fraction of product *i* detected, and V_{CO} the volume fraction of carbon monoxide in the reactant gas.

3 Results

3.1 Physical and Chemical Characteristics

3.1.1 Elemental Composition

Table 1 lists the surface and bulk S/Mo mole ratios. EDS determined the surface S/Mo mole ratio. Total sulfur analysis determined the bulk S/Mo mole ratio, assuming that only S and Mo constituted the MoS_2. This table shows that the bulk and surface S/Mo mole ratios are close to 2, which is the stoichiometric S/Mo mole ratio of MoS_2, and that the S/Mo ratio is not significantly dependent on the preparation conditions.

Table 1 Bulk and surface S/Mo mole ratios of the MoS_2 catalysts with the preparation conditions

Catalyst name	Preparation condition		Bulk S/Mo mole ratio	Surface S/Mo mole ratio
	Pressure (bar)	Temperature (°C)		
S_05_350	5	350	2.02	1.99
S_10_350	10	350	2.01	1.97
S_20_350	20	350	1.96	2.02
S_40_300	40	300	1.90	1.99
S_40_350	40	350	2.10	2.05
S_40_400	40	400	2.04	2.02

3.1.2 X-ray Powder Diffraction

Figure 3 shows the XRD patterns of MoS_2 prepared at various elevated pressures (5–40 bar) at a temperature of 350 °C. As broad XRD peaks generally result from the presence of relatively less crystalline materials, the XRD patterns in Fig. 3 show that only the MoS_2 phase exists, and particles of the MoS_2 catalyst are present in a relatively less crystalline form, which is not clearly affected by the preparation pressure. A similar MoS_2 structure was observed in those prepared by the thermal decomposition of ATTM [38]. It was also reported that the relatively less crystalline MoS_2 has a disordered structure, in which the (0 0 2) planes are stacked to build a few layers [34]. Furthermore, the relatively less crystalline MoS_2 is known to be highly active for catalytic reactions [17, 20].

As shown in Table 2, the slab height calculated by Scherrer's equation [22, 23, 38] using FWHM (full width at half maximum) of the peak corresponding to the (0 0 2) plane and the number of the layers stacked in MoS_2, decreases with increasing the preparation pressure. The average height of the crystallites of crystalline MoS_2 can be estimated from the diffraction peak for the (0 0 2) plane in the low 2θ range, while the length of the basal plane can be estimated from the ones for the (1 0 0), (1 0 1), or (1 1 0) [8, 22]. However, the length of the basal plane of relatively less crystalline MoS_2 cannot be easily estimated from XRD patterns due to random defects, an overlap of peaks, and the folding of basal planes [8, 22, 39]. Moreover, it is well known that an increase in the FWHM indicates a decrease in the stacking and crystallite size (H), where the number of the stacked layer (n) is calculated by n = H/6.17 (H in Å) [22]. In general, the height of the MoS_2 peaks increases, and the width

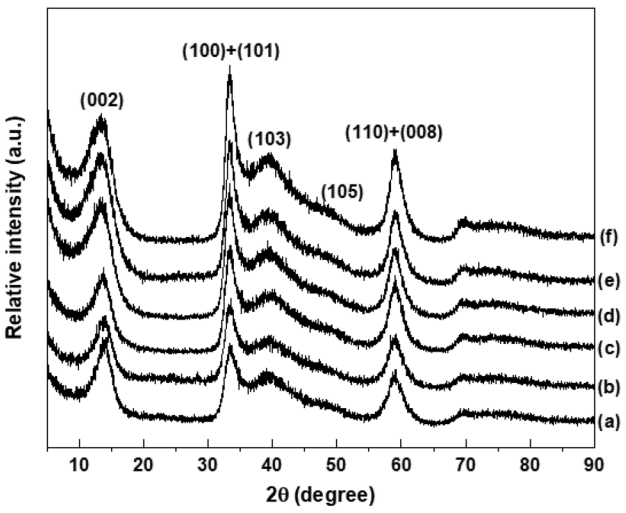

Fig. 3 X-ray diffraction patterns of the MoS_2 catalysts: *a* S_05_350, *b* S_10_350, *c* S_20_350, *d* S_40_300, *e* S_40_350, and *f* S_40_400

Table 2 Physical and chemical characteristics of the prepared MoS_2 catalysts

Catalyst name	Slab height (nm)[a]	The number of stacked (0 0 2) planes[b]	BET surface area (m^2/g)	Average pore volume (cm^3/g)	Average pore size (nm)	Surface Mo^{4+} mole ratio to total Mo[c]	Surface SO_4^{2-} mole ratio to total S[c]
S_05_350	2.37	3.8	35.26	0.02	2.53	0.913	0.083
S_10_350	2.29	3.7	112.08	0.09	3.07	0.892	0.136
S_20_350	2.18	3.5	176.74	0.17	3.78	0.920	0.168
S_40_300	1.72	2.8	306.70	0.59	7.68	0.918	0.086
S_40_350	1.88	3.0	346.91	0.85	9.81	0.933	0.094
S_40_400	2.07	3.4	273.46	0.61	9.04	0.941	0.093

[a]Estimated by Scherrer's equation at the peak of the XRD patterns corresponding to the (0 0 2) plane of MoS_2

[b]Calculated by an equation of the slab height in Å/6.17

[c]Estimated of the XPS spectra

becomes narrower by increasing the preparation temperature at a preparation pressure of 40 bar. This phenomenon is in agreement with the results of Afanasiev [9], Daage and Chianelli [22], and Iwata et al. [23], where the particles of MoS_2 can grow in the height of MoS_2 slab by increasing preparation temperature.

3.1.3 Scanning Electron Microscopy (SEM)

All MoS_2 catalysts prepared in this study are present in agglomerates of irregular nano-sized particles (see Fig. 4). The particles of the MoS_2 catalyst prepared at a preparation pressure of 5 bar are fused together to form the

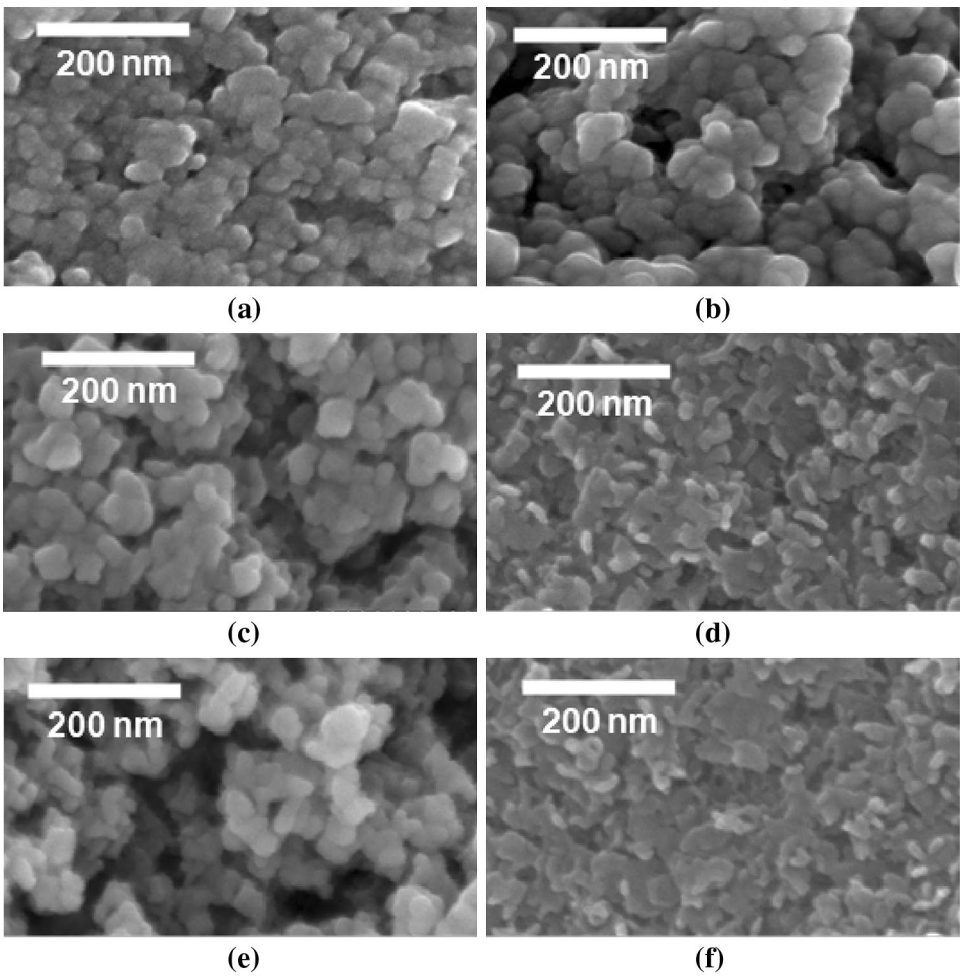

Fig. 4 SEM photomicrographs of the MoS_2 catalysts: **a** S_05_350, **b** S_10_350, **c** S_20_350, **d** S_40_300, **e** S_40_350, and **f** S_40_400

agglomerates. As the preparation pressure is increased from 5 to 40 bar, the fused portion gradually disappears, indicating that a high preparation pressure could reduce the extent of agglomeration. In studies of MoS_2 prepared by using a mechanically pressurized precursor in the aqueous phase, the catalyst consisted of irregularly rounded particles, and the degree of agglomeration was significantly reduced by the pressurization [35, 40]. Thus, it is expected that high pressure of H_2 gas in the preparation facilitates the segregation of MoS_2 particles from each other.

On the other hand, an increase in preparation temperature from 300 to 400 °C at 40 bar intensifies the fusion of the particles to result in compact agglomerates (see Fig. 4). Calais et al. [39] also reported that an increase in decomposition temperature from 400 to 700 °C rapidly sintered the particles of MoS_2 during thermal decomposition.

3.1.4 Transmission Electron Microscopy (TEM)

As all samples show similar images, a representative of the low resolution TEM images is exhibited for the sample prepared at 350 °C and 5 bar in Fig. 5a. The shape of the particles in the low-resolution image of Fig. 5a can be termed "rag-structure", based on the observation by Chianelli et al. [1]. On the other hand, the high-resolution images of Fig. 5b–d reveal that the MoS_2 particles involve a lattice fringe with a spacing of 0.65 nm, which is quite close to the 0.62 nm one for crystalline MoS_2 (2H–MoS_2) [1, 20, 39]. Furthermore, bent fringes with multi-layered structures become severe with an increase in the preparation pressure. It was reported that several MoS_2 layers were folded and disordered in the rag-structure [1]. However, variation of the preparation temperature between 300 and 400 °C at 40 bar does not significantly affect the shape of the fringes. Even though it was reported that a bent lattice fringe becomes straight at a temperature above 700 °C [9], it is supposed that the preparation temperatures in this study are too low to straighten the bent fringe.

3.1.5 N_2 Adsorption–Desorption Isotherms

The N_2 adsorption–desorption isotherms of the MoS_2 catalysts in Fig. 6 show that an increase in preparation pressure from 5 to 40 bar can sharply raise the amounts of N_2 adsorbed on MoS_2. Furthermore, it is noteworthy that the type of the N_2 adsorption–desorption isotherms in Fig. 6 is dependent on the preparation pressure. According to the IUPAC classification standard [41], the MoS_2 prepared at 20 bar has a Type IV N_2 adsorption isotherm with a Type H2 hysteresis loop, whereas that prepared at 40 bar has a Type II N_2 adsorption isotherm with a Type H3 hysteresis loop. It has been well known that a Type IV N_2 isotherm is the typical characteristic of mesoporous solids such as industrial adsorbents [41, 42], and a Type II N_2 isotherm is normally obtained from macroporous adsorbents [41]. In addition, a Type H2 hysteresis loop has been obtained in aggregates or agglomerates of spheroidal particles [42] having pores with a nonuniform size or shape [42]. A Type H3 hysteresis loop has been normally observed in aggregates or agglomerates of plate-like or edged particles giving rise to slit-shaped pores with nonuniform size or shape [42]. Therefore, it is found that the MoS_2 prepared at 20 bar exists as aggregates with mesopores of nonuniform size or shape, whereas the one prepared at 40 bar has some macropores as well as mesopores.

The average pore size and BET surface areas summarized in Table 2 are acquired from the N_2 adsorption–desorption isotherms of the MoS_2 samples. The average pore size and BET surface area significantly increase as the preparation pressure is increased. However, in the variation of preparation temperature at 40 bar, the average pore size and BET surface area are maximized at a temperature of 350 °C.

3.1.6 X-ray Photoelectron Spectroscopy (XPS)

The oxidation states of Mo and S on the surface of the prepared MoS_2 are found from the Mo 3d and S 2p XPS spectra. Since the shapes of XPS spectra are similar for all catalysts, the representing spectra of the one prepared at 350 °C and 40 bar are shown in Fig. 7, including the deconvolution of the peaks for Mo 3d and S 2p. The Mo 3d XPS spectrum is deconvoluted using an intensity ratio of 2/3 and a splitting of 3.1 eV between two Mo 3d peaks ($3d_{5/2}$ and $3d_{3/2}$) [43], employing a combination of 20% Gaussian and 80% Lorentzian distributions. On the other hand, the S 2p XPS spectrum is deconvoluted using an intensity ratio of 2/1 and a splitting of 1.2 eV between two S 2p peaks ($2p_{3/2}$ and $2p_{1/2}$) [43], employing a combination of 35% Gaussian and 65% Lorentzian distributions.

In Fig. 7a, two deconvoluted peaks at 229.1 and 232.2 eV correspond to Mo^{4+} in MoS_2 [43, 44], and those at 231.4 and 234.6 eV to Mo^{6+} in MoS_3 [43]. As the oxidation state of Mo at 230.3 eV of Mo $3d_{5/2}$ peak and 233.4 eV of Mo $3d_{3/2}$ peak is higher than that corresponding to Mo^{4+} and lower than that of Mo^{6+}, it is estimated that the above peaks can be attributed to Mo^{5+} in Mo_2S_5 [43, 45, 46]. According to the study by Wang's research group [45], Mo_2S_5 could exist as an intermediate product between MoS_2 and MoS_3 in MoS_2 preparation by heating an ATTM solution. On the other hand, the peak at 226.3 eV is allocated for S 2s of MoS_2, based on the research by Wang et al. [43], and Roy and Srivastava [44].

In Fig. 7b of S 2p XPS spectrum, two S $2p_{3/2}$ peaks at ca. 162.0 eV and ca. 168.6 eV can be attributed to S^{2-} in MoS_2 [43, 44, 47] and SO_4^{2-} species [43, 47], respectively. According to Wang et al. [43], sulfate may remain as a residue when

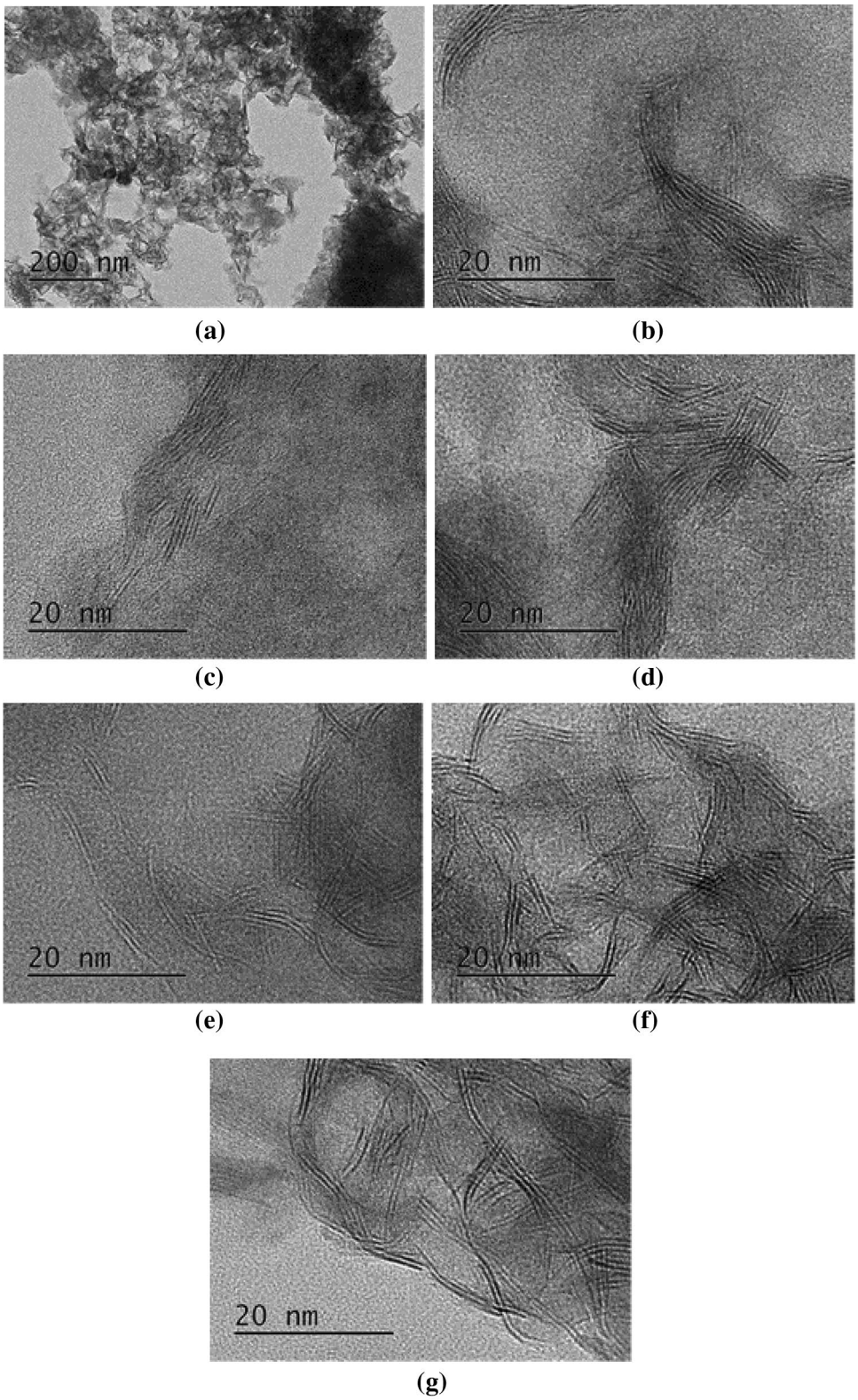

Fig. 5 TEM images of the MoS_2 catalysts: **a** low-resolution image of S_40_300, and high -resolution images of **b** S_05_350, **c** S_10_350, **d** S_20_350, **e** S_40_300, **f** S_40_350, and **g** S_40_400

sulfuric acid is used in MoS_2 preparation. Pathak et al. [46] announced that the existence of the SO_4^{2-} species is related to the bisulfite (HSO^{3-}) and bisulfate (H_2SO^{4-}) residues in the precipitates formed in the MoS_2 preparation. In addition, the production of the sulfate has been accounted for through the oxidation of the adsorbed H_2S, or low balance sulfur by oxidants such as H_2O or CO_2 [47]. Accordingly, it is postulated that SO_4^{2-} species at about 168.6 eV may be attributed

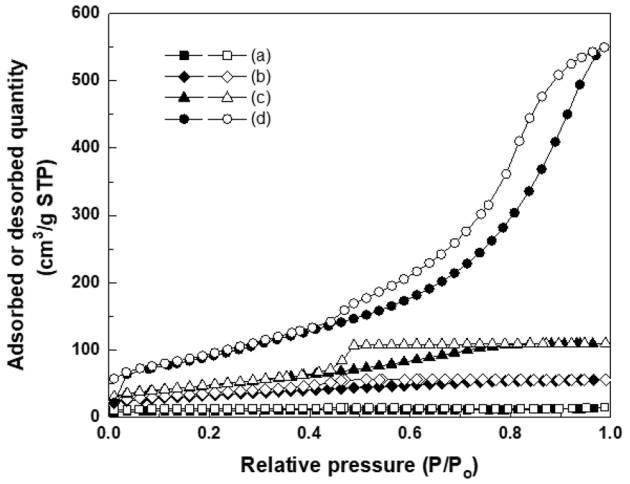

Fig. 6 Nitrogen adsorption–desorption isotherms of the MoS_2 catalysts: The open and closed symbols denote adsorption and desorption, respectively; *a* S_05_350, *b* S_10_350, *c* S_20_350, and *d* S_40_350

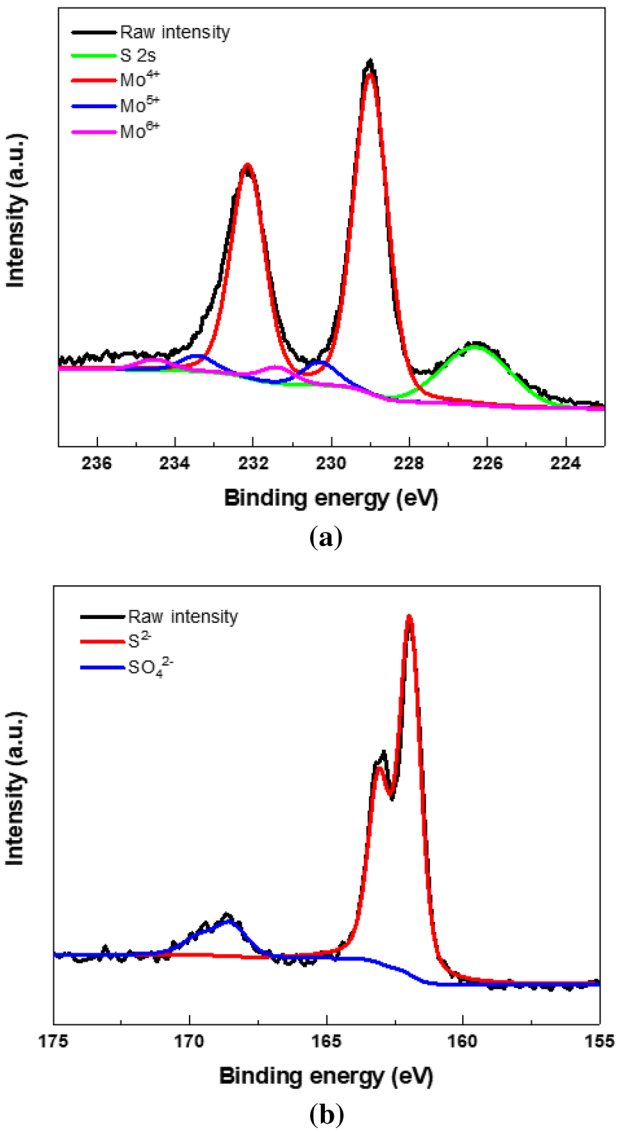

Fig. 7 Representative XPS spectra of the MoS_2 catalyst (S_10_350) with the deconvoluted peaks: **a** Mo 3d and **b** S 2p

to the sulfate residue formed by the oxidation of a part of H_2S produced from ATTM in an aqueous phase in H_2 during the hydrothermal synthesis of MoS_2.

The mole ratios of Mo^{4+} to total Mo and SO_4^{2-} to the sum of SO_4^{2-} and S^{2-} are summarized in Table 2. Although the Mo^{4+} mole ratios are not much different between the catalysts, it is worth noting that the ratio is slightly increased by increasing the preparation pressure and temperature. Thus, the high pressure and temperature in the preparation might lead to favorably transform Mo^{6+} of ATTM as a precursor into Mo^{4+} of MoS_2. Moreover, the sulfate residue seems to be the highest in the MoS_2 catalyst prepared at 350 °C and 20 bar, which might imply that most H_2S adsorbed at the preparation conditions could be likely oxidized.

3.1.7 CO-Temperature Programmed Desorption (TPD)

In the CO-TPD profiles of the MoS_2 samples shown in Fig. 8, three CO desorption peaks are observed: the first (Peak 1) is located at approximately 100 °C, the second (Peak 2) between 600 and 700 °C, and the third (Peak 3) at approximately 780 °C. In general, the number of desorption peaks represents the number of adsorption sites, which have different adsorption enthalpy and desorption activation energy [48]. In a comparison between Peak 1 and Peak 2 of all catalysts, Peak 1 is relatively weaker than Peak 2 in intensity, which means that most of the CO is strongly chemisorbed in the MoS_2 catalysts. Peak 3 is observed only in the CO-TPD of the catalyst prepared at 40 bar, which implies that the adsorption site corresponding to Peak 3 can more strongly adsorb CO than that of Peak 2.

The amount of CO desorption corresponding to Peak 1 increases with an increase in the preparation pressure, which is indicative of the enhancement of weak adsorption of CO species [49]. In addition, the overall CO desorption of Peak 2 and Peak 3 rises in amount with increasing preparation pressure, inducing the improvement of the catalytic activity of the MoS_2. It has been suggested that the strong CO adsorption site is associated with the sulfur vacancy as a catalytic active site [50].

3.1.8 H_2-Temperature Programmed Reduction (TPR)

In Fig. 9 for the H_2-TPR profile of the MoS_2, H_2 consumption occurs mainly at a low temperature of approximately 230 °C. It can be seen that H_2 consumption increases with an increase in the preparation pressure (see Fig. 9a), and it

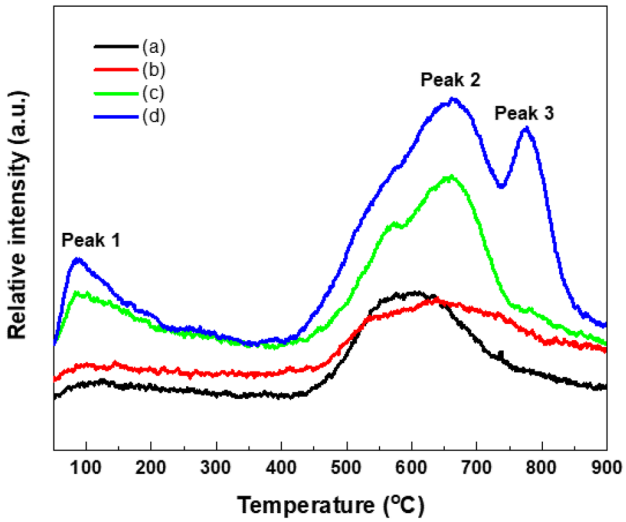

Fig. 8 CO-TPD profiles of the MoS_2 catalysts: *a* S_05_350, *b* S_10_350, *c* S_20_350, and *d* S_40_350

is maximized at 350 °C with varying preparation temperatures (see Fig. 9b). According to Jacobsen et al. [13] and Mangnus et al. [51], the appearance of H_2-TPR peaks in the low temperature range is due to the sulfur weakly bonding to the surface of the catalyst, or extra sulfur present. In a H_2-TPR study of transition metal sulfides, a peak in the low temperature domain was addressed due to the weakly bonded sulfur related to the surface reaction, whereas that in the high temperature one was due to a bulk reduction [52]. In the same study, the weakly bonded sulfur could produce coordinated unsaturated sites (CUS), which might be related to the catalytic activity of transition sulfides. Li et al. [53] proposed that sulfur vacancies could be formed by the formation of H_2S through the reaction of S with H_2 on the surface of MoS_2. Hence, high pressure and a temperature of 350 °C in the preparation possibly develops the formation of sulfur vacancies for H_2 consumption.

3.2 Catalytic Performance

Figure 10 shows CO conversion profiles against reaction time in the methanation reaction over the MoS_2 catalysts. In general, maximum CO conversions of the catalysts are reached within 90 min of reaction time, and conversions after 90 min monotonically decrease with reaction time. In Fig. 10, for the catalysts prepared at 350 °C, the decreasing rate of CO conversion after 90 min is more significant in the catalyst prepared at 5 bar than those at 20 and 40 bar. On the other hand, in the catalysts prepared at 40 bar with varying temperatures, the decreasing rates of CO conversion after 90 min are much lowered, especially at 400 °C. To compare the catalysts in catalytic performance, the CO conversions between 3 and 7 h are averaged and summarized in Table 3.

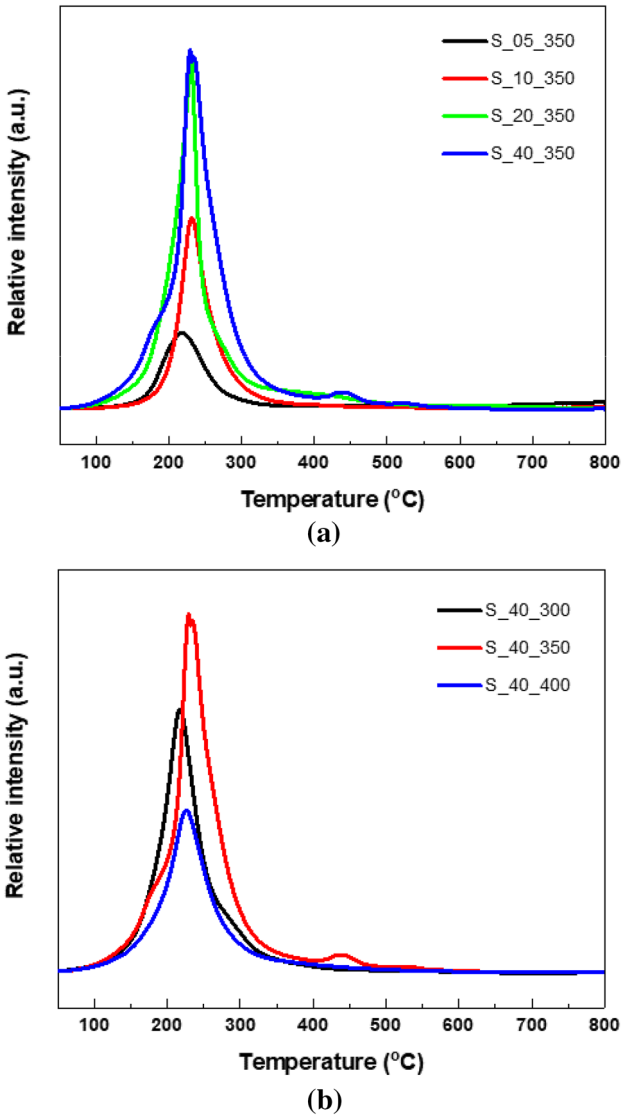

Fig. 9 H_2-TPR profiles of the MoS_2 catalysts: **a** variation of preparation pressures (5–40 bar) at 350 °C, and **b** variation of preparation temperatures (300–400 °C) at 40 bar

It is apparent that the catalytic performance of the MoS_2 catalysts in CO conversion is improved by increasing the preparation pressure. Furthermore, the methanation reactivity of catalysts is high at preparation temperatures in the order of 350, 300, and 400 °C. Therefore, the results suggest that the optimum conditions for MoS_2 preparation are 350 °C and 40 bar in terms of CO conversion.

4 Discussion

The hydrothermally prepared MoS_2 catalysts are formed in bent fringes with a nano-sized slab by stacking the (0 0 2) planes, which is confirmed by the results of TEM and XRD.

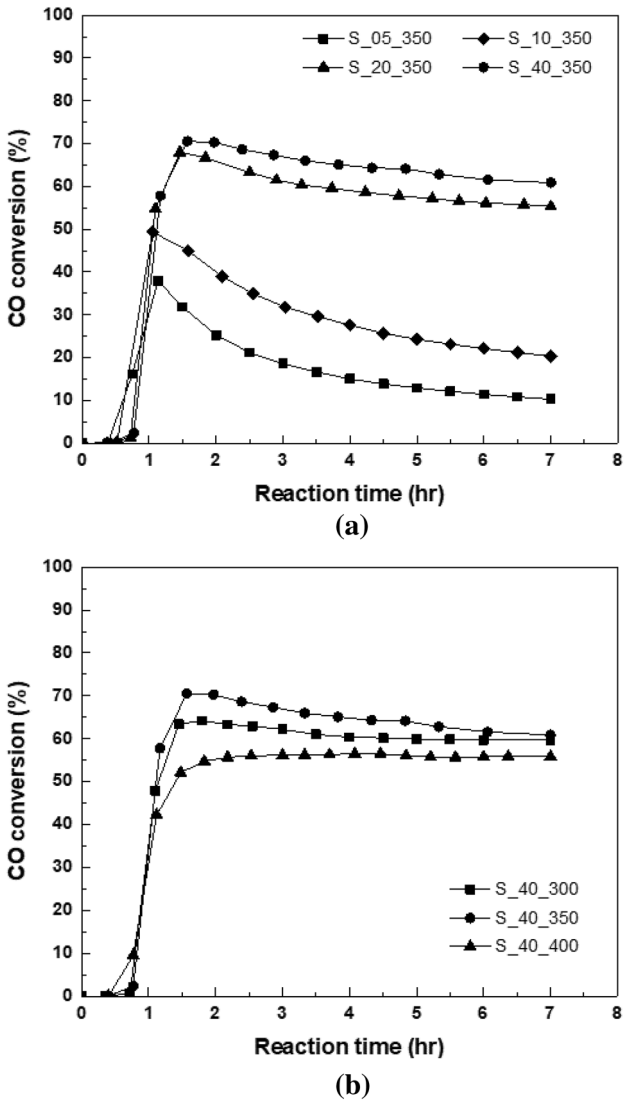

Fig. 10 CO conversions of the MoS_2 catalysts in the methanation: **a** variation of preparation pressures (5–40 bar) at 350 °C, and **b** variation of preparation temperatures (300–400 °C) at 40 bar

The nano-sized particles are chemically composed of MoS_2, with some Mo_2S_5 and MoS_3, where a little of SO_4^{2-} is also present on the surface. Thus, some Mo^{6+} of ATTM might be incompletely decomposed to Mo_2S_5 and MoS_3 that are probably located on the curved edges of the bent fringes during the preparation. In addition, as the existence of sulfur vacancies in the catalysts is observed in CO-TPD and H_2-TPR, the surface SO_4^{2-} is postulated to be associated with the vacancies. The sulfur in Mo_2S_5 and MoS_3 might be depleted by reacting with H_2 to H_2S, which leaves a sulfur vacancy on the surface. After the synthesized catalysts are exposed to the atmospheric environment, it is expected that the vacancy could get oxidized to SO_4^{2-} on the surface. In general, it has been observed that the sulfur vacancy could improve the catalytic activity of MoS_2 [20, 52, 53]. It was also suggested that the sulfur vacancies facilitating the methanation reaction are also involved in the sulfur species weakly bonded to the surface of MoS_2 [20].

The physical properties, such as the shape of the fringes, the BET surface area, and the height of the slab, are greatly dependent on the preparation pressure. Increasing the preparation pressure at 350 °C, it is seen that the curved basal planes of MoS_2 is increased in number, and the slab height is reduced. In addition, high preparation pressure can develop the pore structure, which raises the BET surface area of the MoS_2 catalyst. According to the results of XPS, CO-TPD, and H_2-TPR, more surface Mo^{4+} and sulfur vacancies appear at higher preparation pressures, which probably leads to the improvement of the catalytic performance of MoS_2 catalysts in methanation. Analogously, it was reported that the catalytic activity of MoS_2 for hydrodesulfurization is associated with BET surface area [12, 34]. On the other hand, Iwata's research group proposed that active sites such as sulfur vacancies could exist on the curvature of the basal planes of MoS_2, as well as on the edge planes [17, 23]. Thus, it is suggested that the development of the bent fringes and the pore structure at high preparation pressure could induce the appearance of surface Mo^{4+} and sulfur vacancies in the catalysts, which can provide highly active sites for CO adsorption, H_2 reduction, and the methanation.

Table 3 Summary of the catalytic performance of the prepared MoS_2 catalysts in methanation

Catalyst name	CO conversion (%)	CH_4 concentration (%)	CO_2 concentration (%)	C_2H_6 concentration (%)	C_3H_8 concentration (%)
S_05_350	18.31	6.14	4.16	0.52	0.06
S_10_350	30.31	10.08	8.38	0.93	0.11
S_20_350	59.74	20.37	22.39	2.52	0.29
S_40_300	61.40	18.75	23.23	3.11	0.49
S_40_350	65.60	21.48	25.87	3.07	0.55
S_40_400	55.68	15.04	20.01	2.94	0.53

Conversion and concentrations averaged between 3 and 7 h of the reaction time

Even though the fringe shape does not change much with preparation temperature at a fixed pressure of 40 bar, the fringes slightly grow in slab height with an increase in the preparation temperature. Thus, it is expected that the BET surface area will decrease with an increase in the slab height by the preparation temperature. However, the surface area seems to be maximized at a preparation temperature of 350 °C in this study. In general, it has been reported that an increase in preparation temperature from 350 to 700 °C could decrease the BET surface area of MoS_2 prepared by thermal decomposition of ATTM [9, 23]. Afanasiev [9], in particular, claimed that a preparation temperature between 400 and 700 °C could decrease BET surface area of MoS_2 due to the plugging of the micropores in the catalyst, as well as the growth of the MoS_2 slab. However, as the mole fraction of surface Mo^{4+} in the catalyst increases with an increase in the preparation temperature (see Table 2), it should be noted that the preparation temperature can affect not only the slab height but also the decomposition of ATTM precursor into MoS_2. It has been known that the thiosalt precursor could be incompletely decomposed into MoS_2 at a temperature below 350 °C [34, 45]. Thus, with preparation temperatures at or below 350 °C, the decomposition of the ATTM precursor into MoS_2 could be dominant to enhance the BET surface area by producing the pore structure. On the other hand, for a preparation temperature above 350 °C, the increase in the MoS_2 slab height could primarily cause plugging of pores and lower the BET surface area. Furthermore, such a phenomenon could severely affect the amount of the active sites related to the surface Mo^{4+} species and the sulfur vacancies. As the surface Mo^{4+} is observed to be increasingly present with an increase in the preparation temperature, it is obvious that a high preparation temperature must be beneficial to prompt the decomposition and create the active sites. Nevertheless, the catalytic activity in the methanation drops sharply in the catalyst prepared at 400 °C (see Table 3). Thus, according to the H_2-TPR result showing the maximum incidence of sulfur vacancies in the catalyst prepared at 350 °C, it is considered that the entrances of the pores generated at 350 °C of the preparation temperature could be closed at 400 °C, preventing reactants from getting adsorbed on the active sites.

5 Conclusions

Unsupported MoS_2 catalysts prepared by hydrothermal reaction using ammonium tetrathiomolybdate (ATTM, $(NH_4)_2MoS_4$) show relatively broad XRD peaks, which are the characteristics of less crystalline materials. The particles of the catalysts are formed in the bent fringes by stacking the (0 0 2) planes. Mo^{6+} of the ATTM precursor are mainly transformed into MoS_2, with some Mo_2S_5 and MoS_3 produced during the synthesis. Also, a small amount of the surface sulfur species is present in sulfate form. The increase in preparation pressure results in the increase in the curvature on the basal planes of MoS_2, and a decrease in the degree of stacking of slab related to the crystallite size of MoS_2, which could enhance the BET surface area. It is suggested that the increase in surface Mo^{4+} and sulfur vacancies observed at high preparation pressures could improve the catalytic activity of MoS_2 for methanation. Although the increase in the preparation temperature from 300 to 400 °C could likely decompose the ATTM precursor into MoS_2, a high preparation temperature above 350 °C decreases the BET surface area and the amount of the catalytic active sites, such as sulfur vacancies, available for the methanation reaction. Accordingly, it is suggested that an optimum preparation temperature of 350 °C is required to maximize the catalytic performance for methanation by completing the decomposition of the precursor and securing the accessible active sites.

Acknowledgements We would like to acknowledge the financial support from the R&D Convergence Program (CAP-16-11-KAERI) of NST (National Research Council of Science & Technology) of Republic of Korea.

References

1. Chianelli RR, Prestridge EB, Pecoraro TA, Deneufville JP (1979) Science 203:1105
2. Murray R, Evans BL (1979) J Appl Crystallogr 12:312
3. Afanasiev P, Xia GF, Berhault G, Jouguet B, Lacroix M (1999) Chem Mater 11:3216
4. Gu S, Zhang Y, Yan B (2013) Mater Lett 97:169
5. Feng C, Ma J, Li H, Zeng R, Guo Z, Liu H (2009) Mater Res Bull 44:1811
6. Chen TY, Chang YH, Hsu CL, Wei KH, Chiang CY, Li LJ (2013) Int J Hydrog Energy 38:12302
7. Yoosuk B, Tumnantong D, Prasassarakich P (2012) Chem Eng Sci 79:1
8. De la Rosa MP, Texier S, Berhault G, Camacho A, Yacáman MJ, Mehta A, Fuentes S, Montoya JA, Murrieta F, Chianelli RR (2004) J Catal 225:288
9. Afanasiev P (2010) J Catal 269:269
10. Alvarez L, Espino J, Ornelas C, Rico JL, Cortez MT, Berhault G, Alonso G (2004) J Mol Catal A 210:105
11. Trakarnpruk W, Seentrakoon B (2007) Ind Eng Chem Res 46:1874
12. Alonso G, Berhault G, Aguilar A, Collins V, Ornelas C, Fuentes S, Chianelli RR (2002) J Catal 208:359
13. Jacobsen CJH, Törnqvist E, Topsøe H (1999) Catal Lett 63:179
14. Youchang X, Naasz BM, Somorjai GA (1986) Appl Catal 27:233
15. Soto-Puente M, Del Valle M, Flores-Aquino E, Avalos-Borja M, Fuentes S, Cruz-Reyes J (2007) Catal Lett 113:170
16. Zhang F, Vasudevan PT (1995) J Catal 157:536
17. Iwata Y, Sato K, Yoneda T, Miki Y, Sugimoto Y, Nishijima A, Shimada H (1998) Catal Today 45:353
18. Schweiger H, Raybaud P, Kresse G, Toulhoat H (2002) J Catal 207:76
19. Lobos S, Sierraalta A, Ruette F, Rodríguez-Arias EN (2003) J Mol Catal A 192:203

20. Liu J, Wang E, Lv J, Li Z, Wang B, Ma X, Qin S, Sun Q (2013) Fuel Process Technol 110:249
21. Vasudevan PT, Zhang F (1994) Appl Catal A 112:161
22. Daage M, Chianelli RR (1994) J Catal 149:414
23. Iwata Y, Araki Y, Honna K, Miki Y, Sato K, Shimada H (2001) Catal Today 65:335
24. Pramanik P, Bhattacharya S (1989) J Mater Sci Lett 8:781
25. Mdleleni MM, Hyeon T, Suslick KS (1998) J Am Chem Soc 120:6189
26. Alonso G, Del Valle M, Cruz J, Licea-Claverie A, Petranovskii V, Fuentes S (1998) Catal Lett 52:55
27. Joensen P, Frindt RF, Morrison SR (1986) Mater Res Bull 21:457
28. Del Valle M, Cruz J, Avalos-Borja M, Fuentes S (1998) Catal Lett 54:59
29. Zhan JH, Zhang ZD, Qian XF, Wang C, Xie Y, Qian YT (1998) J Solid State Chem 141:270
30. Tian Y, Zhao X, Shen L, Meng F, Tang L, Deng Y, Wang Z (2006) Mater Lett 60:527
31. Devers E, Afanasiev P, Jouguet B, Vrinat M (2002) Catal Lett 82:13
32. Yoshimura M, Byrappa K (2008) J Mater Sci 43:2085
33. Rueda N, Bacaud R, Lanteri P, Vrinat M (2001) Appl Catal A 215:81
34. Siadati MH, Alonso G, Torres B, Chianelli RR (2006) Appl Catal A 305:160
35. Alonso G, Del Valle M, Cruz J, Petranovskii V, Licea-Claverie A, Fuentes S (1998) Catal Today 43:117
36. Peng Y, Meng Z, Zhong C, Lu J, Yu W, Yang Z, Qian Y (2001) J Solid State Chem 159:170
37. Song X, Ding Y, Chen W, Dong W, Pei Y, Zang J, Yan L, Lu Y (2012) Energy Fuel 26:6559
38. Liang KS, Chianelli RR, Chien FZ, Moss SC (1986) J Non-Cryst Solids 79:251
39. Calais C, Matsubayashi N, Geantet C, Yoshimura Y, Shimada H, Nishijima A, Lacroix M, Breysse M (1998) J Catal 174:130
40. Wang S, Wang Z, Qin J, Wang W, Li W, He D (2011) Mater Chem Phys 130:170
41. Sing KSW, Everett DH, Haul RAW, Moscou L, Pierotti RA, Rouquerol J, Siemieniwska T (1985) Pure Appl Chem 57:603
42. Leofanti G, Padovan M, Tozzola G, Venturelli B (1998) Catal Today 41:207
43. Wang HW, Skeldon P, Thompson GE (1997) Surf Coat Technol 91:200
44. Roy P, Srivastava SK (2006) Thin Solid Films 496:293
45. Wang HW, Skeldon P, Thompson GE (1998) J Mater Sci 33:3079
46. Panigrahi PK, Pathak A (2013) J Nanopart 2013:671214
47. Chen A, Wang Q, Li Q, Hao Y, Fang W, Yang Y (2008) J Mol Catal A 283:69
48. Kolasinski KW (2012) Surface science: foundations of catalysis and nanoscience. John Wiley, Chichester
49. Yin H, Ding Y, Luo H, Zhu H, He D, Xiong J, Lin L (2003) Appl Catal A 243:155
50. Travert A, Dujardin C, Maugé F, Cristol S, Paul JF, Payen E, Bougeard D (2001) Catal Today 70:255
51. Mangnus PJ, Riezebos A, Langeveld AD, Moulijn JA (1995) J Catal 151:178
52. Afanasiev P (2006) Appl Catal A 303:110
53. Li XS, Xin Q, Guo XX, Grange P, Delmon B (1992) J Catal 137:3585

Affiliations

Jae-Myeong Choi[1] · Sung-Hyun Kim[1] · Seung-Jae Lee[2] · Seong-Soo Kim[2]

✉ Sung-Hyun Kim
kimsh@korea.ac.kr

✉ Seong-Soo Kim
sskim@kier.re.kr

[1] Department of Chemical and Biological Engineering, Korea University, 145 Anam-ro, Seongbuk-gu, Seoul 02841, Republic of Korea

[2] Biomass and Wastes Energy Laboratory, Korea Institute of Energy Research, 152 Gajeong-ro, Yuseong-gu, Daejeon 34129, Republic of Korea